

Modulation of Host–Parasite Interactions with Small Molecules Targeting *Schistosoma mansoni* microRNAs

Youssef Hamway,[¶] Kaspar Zimmermann,[¶] Marcel J. J. Blommers, Mariana V. Sousa, Cécile Häberli, Shashank Kulkarni, Susanna Skalicky, Matthias Hackl, Marjo Götte, Jennifer Keiser, Clarissa Prazeres da Costa, Thomas Spangenberg,* and Kamal Azzaoui*



Cite This: *ACS Infect. Dis.* 2022, 8, 2028–2034



Read Online

ACCESS |

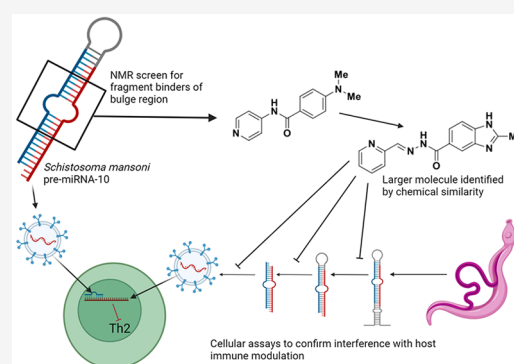
Metrics & More

Article Recommendations

Supporting Information

ABSTRACT: Parasites use different strategies of communication with their hosts. One communication channel that has been studied in recent years is the use of vesicle microRNAs to influence the host immune system by trematodes. *sma*-microRNA-10, secreted from *Schistosoma mansoni*, has been shown to influence the fate of host T-cells through manipulation of the NF- κ B pathway. We have identified low molecular weight tool compounds that can interfere with this microRNA-mediated manipulation of the host immune system. We used a fragment-based screening approach by means of nuclear magnetic resonance (NMR) to identify binders to the precursor of the parasite *sma*-microRNA-10 present in their extracellular vesicles. The small fragments identified were used to select larger molecules. These molecules were shown to counteract the inhibition of NF- κ B activity by *sma*-microRNA-10 in cell-based assays.

KEYWORDS: *microRNA*, *schistosome*, *FBS*, *NMR*, *host–parasite*



Parasitic flatworms of the genus *Schistosoma* are responsible for causing schistosomiasis, a neglected tropical disease affecting 240 million people worldwide.¹ These parasitic worms can persist for decades, necessitating a complex interaction between host and parasite; (i) host factors are utilized for parasite development, and (ii) the parasite modulates the host immune response.² One mechanism of immune modulation is through the use of microRNAs (miRNAs) present in extracellular vesicles (EVs) secreted by the parasites to regulate host immune cells.³ miRNAs are a class of noncoding RNA, implicated in the regulation of several cellular processes through RNA silencing and post-transcriptional regulation of expression. *Schistosoma mansoni*, *S. japonicum*, and *S. hematobium*⁴ each produce a number of different miRNAs⁵ with *S. mansoni* alone producing over 200 of these RNA molecules.⁶

Of these *S. mansoni* miRNAs (*sma*-miRs), *sma*-miR-10-5p, *sma*-miR-bantam-3p, and *sma*-miR-125a-5p were shown to be internalized by host T-cells and to modulate the host immune response^{6–9} and specifically the Th2 immune response that is characteristic of schistosomiasis.¹⁰ In particular, *sma*-miR-10 was found to target MAP3K7 expression and to downregulate NF- κ B activity. NF- κ B targets include the transcription factors *gata3* and AP-1 component *junb*, which play an important role in Th2 signaling through the induction of *il4* expression.^{11–14} This process contributes to the waning of the Th2 response, after 8 weeks, that is associated with chronic parasitic

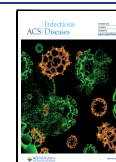
infections and occurs despite the fact that the infection persists and the parasite is not cleared.¹⁵

With *S. mansoni* miRNAs being identified as a key regulator of this process, we were interested in targeting them with the intention of rescuing NF- κ B activity and ultimately reinstating Th2 responsiveness. The goal of this study is to target pre-miRNA with small molecules to prevent its processing and the formation of the mature miRNA, produced during translational expression of the mRNA. With this in mind, we used computational tools to evaluate miRNA precursors for their ability to form a bulge region favorable for small molecule binding. Indeed, structurally labile regions such as bulges, internal loops, and mismatches are usually observed in different RNA families and are potential binding sites for small molecules.

We selected pre-miRNAs to evaluate potential binding sites. It should be noted that the nucleotides that make up these sites are also present in pri-miRNA and double-stranded miRNA, which are loaded into Ago2. RNA binding proteins such as

Received: July 8, 2022

Published: September 13, 2022



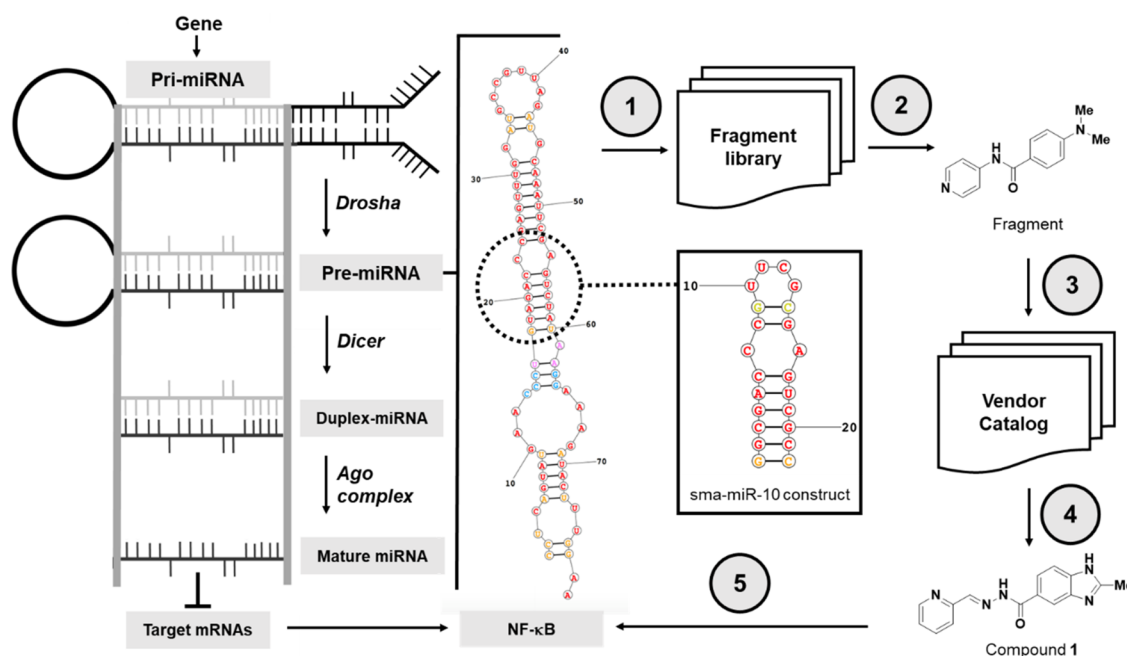


Figure 1. miRNA biogenesis (left). Cascade used to identify small molecules interacting with pre-miRNA sma-pre-miR-10-5p present in the extracellular vesicles of schistosomes to study the host–parasite interaction. (1) Pre-miRNA construct selected for NMR screening (bulge region indicated by dotted circle). (2) Screening by NMR of the fragment library (768 fragments). (3) Selection of molecules by chemical similarity from the vendor catalog. (4) Screening by NMR of the catalog selected molecules (50 molecules). (5) Test compounds in cellular assays.

Drosha, Dicer, and Ago2 act in several stages of the maturation process. The steps that might be inhibited by the binding of a small molecule to RNA would affect loading into the various proteins, RNA cleavage, and finally the release of the sense strand to allow loading of the mRNA into the RISC complex. In other words, a small molecule that binds to one of the sites in pre-miRNA would potentially interfere at several stages of maturation and ultimately modulate the lifetime of the mRNA. At the molecular level, the binding of a small molecule to RNA affects local RNA structure and dynamics, resulting in a change in the interactions with proteins involved in miRNA processing.

In silico prediction of the pre-miRNA secondary structure can provide a first indication of which regions of the pre-miRNA can be targeted, and nuclear magnetic resonance (NMR) is a powerful complementary tool to confirm the secondary structure.

To propose a suitable parasite miRNA target with the knowledge that a number of *Schistosoma* miRNAs have roles in host–pathogen interactions,¹⁰ the available pre-miRNA sequences from *S. mansoni* were downloaded from miRBase¹⁶ and their secondary structures were predicted using previously described tools.^{17,18} In many of the available predicted secondary structures of the pre-miRNAs, the regions with a potential binding pocket containing more than five nucleotides are very flexible and most likely not suitable for ligand binding. It appeared that only a small number of pre-miRNAs were predicted to display potential binding pockets with lower flexibility, such as sma-miR-10, sma-miR-124, and sma-miR-125a, and these were selected for further analysis.

Different RNA constructs were synthesized (Microsynth, Switzerland) and evaluated by ¹⁹F-NMR using a set of 101 fluorinated fragment compounds to select the most suitable construct for a more extended ¹H NMR screening. The sequence of potential binding pockets was inserted into small

RNA hairpins with an ultrastable UUCG loop on one side and a C-G clamp sequence on the other (Figure S1). This allowed us to validate the secondary structure prediction and screen the binding sites individually. For these miRNAs, seven potential binding sites were evaluated by 1D NMR of imino protons to verify folding and by fragment screening using ¹⁹F relaxation (Figure S2, Table S1). It was recently shown that ¹⁹F screening can be applied to RNA to assess the druggability of the RNA targets.^{19,20}

Not only is sma-pre-miR-10 biologically relevant,¹⁰ but also in the proof-of-concept ¹⁹F screen, it showed the highest hit rate for the RNA construct of the sma-miR-10 binding site. In addition, the ¹H NMR spectrum of the imino protons with narrow and well-dispersed resonances showed that the RNA oligonucleotide had a very homogeneous structure (Figure S2). Consistent with these observations, the latter was selected for the larger screen (Figure 1), in which we used a poised fragment library to run a ¹H NMR screen of 768 compounds.^{21,22} It is noted that this library was also validated by screening several other RNAs and resulted in many hits.²³ The secondary structure of the chosen RNA target as well as the hit identification workflow is shown in Figure 1.

Fragments are small and excellent to search the chemical space for chemical scaffolds that bind to the target of choice. Our fragment screening with ligand-observed 1D NMR resulted in 7 hits that were validated by RNA-observed 2D NMR experiments (Table S2). It could be shown that the selected fragment indeed binds to the chosen binding site and not to the loop. Larger compounds, containing these preferred chemical scaffolds, were selected ($n = 50$) from a commercially available catalog of compounds (SPECS, The Netherlands) and screened for binding to the RNA construct. In this follow-up screen, we were able to identify compound 1 (MW 279.3 g/mol) shown in Figure 1 to bind to the RNA construct. Due to the presence of a hydrazine moiety, compound 1 contained

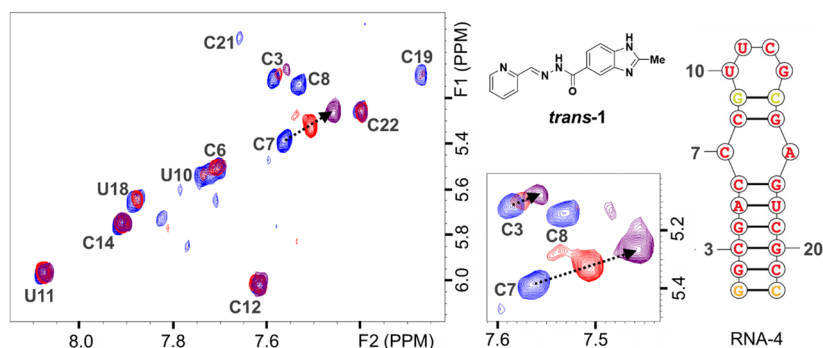


Figure 2. 2D total correlation spectroscopy (TOCSY) NMR fingerprints of the RNA oligonucleotide containing the target binding site of sma-pre-miR-10. The nucleotide sequence and chemical structures of fragment and compound hits are shown in Figure 1. The observed CSP of the RNA at position C7 and not at positions U10, U11, and C12 indicates that the hits bind to the AC mismatch and not to the loop.

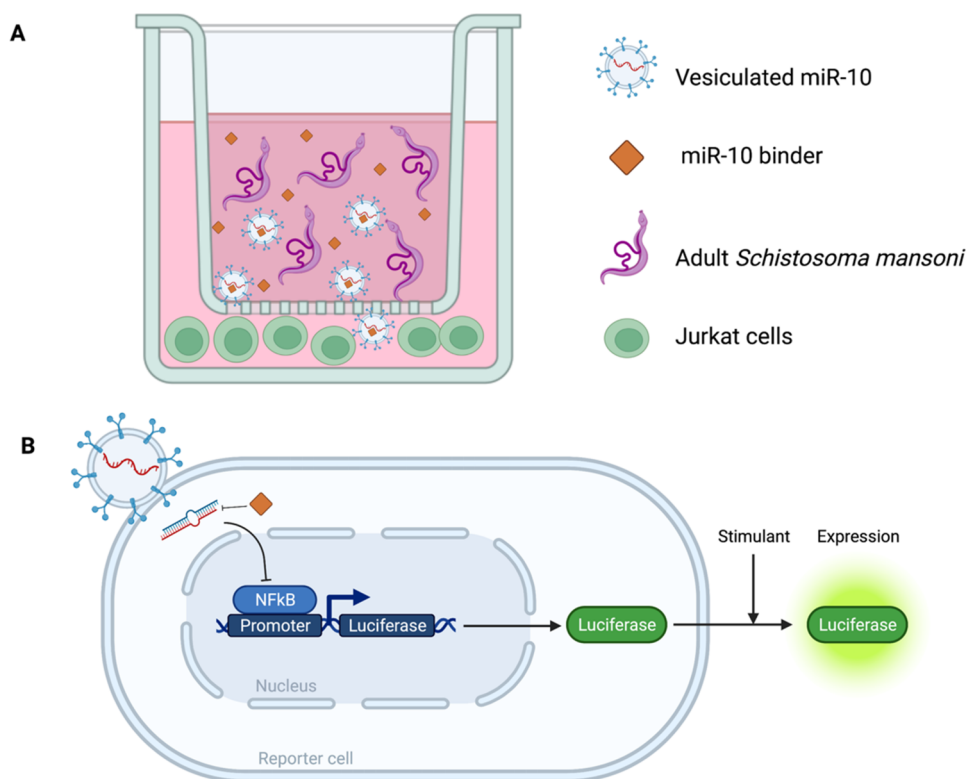


Figure 3. Schematic of the experimental approach. (A) Small molecules bind sma-miR-10 produced by adult *Schistosoma mansoni*, preventing the sma-miR-10-mediated inhibition of the NF- κ B activity level in host T-cells; in the experimental model, this is measured using a Jurkat NF- κ B luciferase reporter cell line (B).

two isomers with different chemical shifts (*trans*-1; *cis*-1) with a high-density population of the *trans*-1 form, which binds to the RNA and was validated by 2D NMR (Figure 2). Other analogues of 1 with a variation of the pyridyl nitrogen's position were synthesized (2 and 3). Each of them was subjected to binding studies by 1D NMR to fully validate them (see the Supporting Information). Finally, compound *trans*-1 was also subjected to a full-length sma-pre-miR-10 binding study, and significant CSPs (chemical shift perturbations) and line broadening of their resonances were observed upon addition of the full-length RNA.

Binding of small molecules to the bulge, located in the middle of the double-stranded region, stabilizes this region and, therefore, can affect multiple processes of RNA–protein interactions; it is difficult to predict whether the binding event will have agonistic or antagonistic effects on the biological

function of sma-miR-10. Therefore, the next step was to confirm this effect using a phenotypic cellular assay.

To study the effect of the binders on the worms, we exposed the parasites to compound *trans*-1 for several days, and the mature sma-miR-10 was quantified in the medium as well as in the whole organism.

Compound *trans*-1 was incubated with *S. mansoni* adult worms at various concentrations, and no lethality or reduction in viability could be observed up to a concentration of 20 μ M. When the compound *trans*-1 was incubated at 0.2, 2, and 20 μ M, the levels of sma-miR-10-5p in the worms and supernatant showed a nonsignificant trend of decreasing by up to 20% with an increase in concentration after 96 h (Figure S3). No trends were observed in secreted levels of sma-miR-10-5p. A potential reason for this observation is the limited cell permeability of the compound (Table S3).

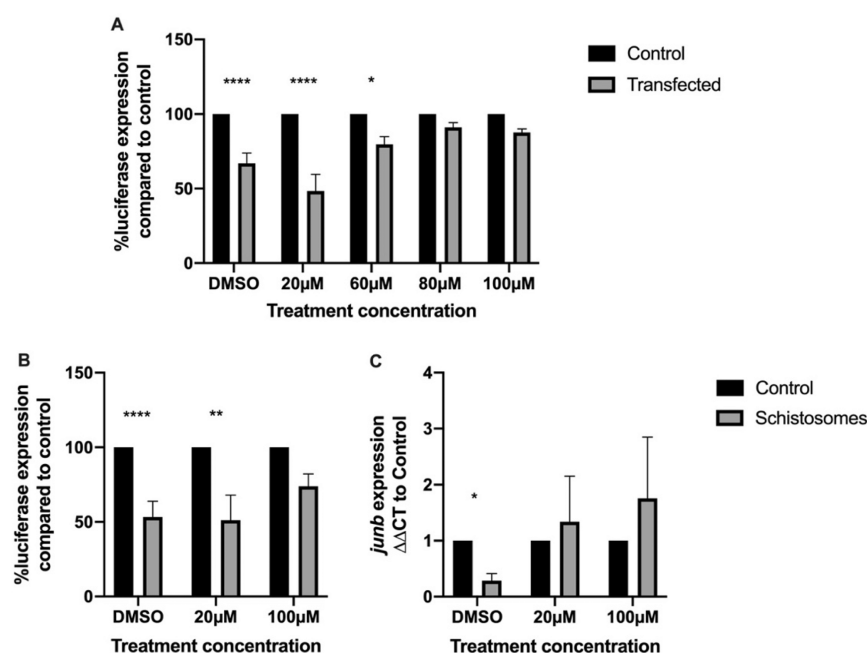


Figure 4. Cellular assays to investigate the phenotypic effect of compound *trans*-1 on sma-miR-10 activity. NF- κ B luciferase reporter Jurkat cells were transfected with 0.25 μ M duplexed sma-miR-10 using DOTAP (1,2-dioleoyl-3-trimethylammonium-propane) as a liposomal transfection agent or exposed to 5–10 *Schistosoma mansoni* via a 0.4 μ m transwell. These cells and control untreated cells were both treated with the above compounds at the indicated concentrations or with DMSO (20 μ L). DOTAP without duplex sma-miR-10 was also added to the DMSO-treated cells with no effect on luciferase expression. Both transfection (A) and worm exposure (B) led to a 50% reduction in luciferase expression, which was restored in a dose-dependent manner by each of the compounds. Additionally, RNA was extracted from cells in the same experiment as in (B), and *junb* RNA expression was measured using qRT-PCR (C) with a similar recovery as that in the luciferase assay. Mean + SEM. Multiple unpaired *t* tests: * $P \leq 0.05$, ** $P \leq 0.01$, *** $P \leq 0.001$, and **** $P \leq 0.0001$. (A, B) $n = 3$. (C) $n = 2$.

After confirmation that the chemical series represented by *trans*-1 led to a downregulation of sma-miR-10-5p in treated worms, the next step was to test if this downregulation counteracted the described function of sma-miR-10-5p of the NF- κ B modulation. A Jurkat NF- κ B luciferase reporter cell line was used to assess the NF- κ B activity in cells directly transfected with duplexed sma-miR-10 or exposed to *S. mansoni* via a ThinCert cell culture insert (Figure 3).

Both transfection with duplex sma-miR-10 and *S. mansoni* exposure led to an expected decrease in NF- κ B activity (Figure 4) of around 50%. The addition of compound *trans*-1 reversed the NF- κ B activity with a dose-dependent increase observed. The two highest doses tested, 80 and 100 μ M, resulted in a near-complete restoration of the NF- κ B activity. This outcome was evident in both the transfection experiment and the *S. mansoni* exposure experiment. To assess the downstream effects of this phenotype, we investigated the NF- κ B target *junb*, which is implicated directly in Th2 regulation and is dynamically-expressed in unstimulated Jurkat cells, unlike Th2 master regulator *gata3*. Total RNA was extracted from the schistosome-exposed cells and *junb* expression, measured by qRT-PCR. The results are in line with those of NF- κ B activity with a reduction in expression evident upon exposure to schistosomes, followed by a dose-dependent recovery of expression. Due to the complex regulation of the *junb* expression,²⁴ some more variability can be observed in these experiments as compared to the direct measurement of the NF- κ B activity. Modulation of the NF- κ B signaling could also be observed for the other isomers of 1 (Figure S4). As compound *trans*-1 and its analogues have a rather low permeability, this may limit the absorption/concentration in the worm/cells (Table S3).

In conclusion, in this study, we aimed to shed light on the *S. mansoni* persistence strategy of immunomodulation using miRNAs. We have identified that these miRNAs are able to form a structural labile region favorable for small molecules to bind as determined by ¹H NMR. First, a fragment-based library was screened with ¹⁹F-NMR on a sma-miR-10 construct to identify binding fragments, allowing us to subsequently select larger molecules from commercially available libraries. Ultimately, binders were studied on sma-miR-10 and were able to counteract sma-miR-10-dependent NF- κ B modulation in human Jurkat cells, as demonstrated by both worm exposure and transfection experiments. The effect of the small molecules in both experimental setups suggests that the compounds can act either on the bulge region in the miRNA precursor (as screened), preventing its maturation, or on the duplex miRNA, interfering with release of the sense strand, as the transfection experiments would suggest. This is representative of the *in vivo* scenario, where miRNAs secreted by schistosomes were able to modulate NF- κ B activity in T-cells.¹⁰ This effect was previously demonstrated to specifically downregulate the Th2 lineage determination of these T-cells, interfering with this immune response to parasitic infection. This interference is hypothesized to be responsible, at least in part, for the hallmark reduction in the Th2 response that is evident in the course of schistosomiasis. The reduced responsiveness takes place despite the persistence of the infection, and it is in fact thought to enable this persistence. Therefore, the prospect that the downregulation of this response is initiated by *Schistosoma* in order to facilitate its own persistence and survival is an appealing one. Thus, the tool compounds discovered in this study are potential immune response enhancers with the possibility of sustaining the Th2 response beyond the initial 8-

week phase and enabling clearing of the infection. Enhanced Th2 responses have already been posited as a source of antischistosome protective immunity, though it should also be noted that strong Th2 responses have also been demonstrated to result in increased immunopathology.^{25–27} More generally, these compounds offer a proof-of-concept as miRNA-targeting small molecules that yield a distinct phenotype.

METHODS

NMR Spectroscopy. All spectra were recorded on a Bruker 600 MHz Advance spectrometer equipped with a 5 mm QNP cryoprobe and a SampleCase sample changer.

Imino proton spectra were measured from 100 μM RNA dissolved in 50 mM phosphate buffer, pH 6.0, and 10% D_2O . The water suppression was achieved through excitation sculpting. Spectra were recorded at different temperatures (5–35 $^\circ\text{C}$).

Samples for ^{19}F fragment screening contained 30 μM fragments and 20 μM RNA dissolved in 50 mM phosphate buffer, pH 6.0, and 10% D_2O . Fragments were measured in mixtures of 30 compounds containing at least one ^{19}F atom. T_2 relaxation was measured using a Carr–Purcell–Meiboom–Gill (CPMG) relaxation pulse train with time lengths of 40, 80, 160, and 320 ms.

Samples for ^1H NMR fragment screening contained 50 μM fragments and 5 μM RNA dissolved in 50 mM phosphate buffer, pH 6.0, and 10% D_2O . 1D spectra were acquired with excitation sculpting water suppression and an additional perfect echo pulse to correct artifacts caused by J modulation of the resonances of the small molecules.²⁸ The CSPs observed by the ligand were used along with the observed line broadening (T_2) to identify hits. Hits were validated by preparing samples of 50 μM RNA and 500 μM of compound dissolved in 50 mM phosphate buffer, pH 6.0, and 100% D_2O . The TOCSY spectrum²⁹ was measured with a 50 ms cecoupling in the presence of scalar interactions (DIPSI) spin-lock pulse and acquired with $400 \times 2\text{k}$ data points in T1 and T2.

The TOCSY spectrum was assigned in conjunction with nuclear Overhauser effect spectroscopy (NOESY) spectra recorded in H_2O and D_2O as described before.³⁰

Jurkat Cell Assays. For all experiments, 3×10^5 Jurkat NF- κB luciferase reporter cells (BPS bioscience, #60651) were seeded in a 6-well plate with 3 mL of RPMI 1640 medium (ATCC modification, Gibco, #A1049101) supplemented with 10% FCS, 100 U/mL penicillin, and 100 $\mu\text{g}/\text{mL}$ streptomycin and incubated overnight before further manipulation.

For the transfection experiments, 0.25 μM of duplexed 5' phosphorylated sma-miR-10-5p/3p was vesiculated in 30 μL of DOTAP (1,2-dioleoyl-3-trimethylammonium-propane) (Roche, #11202375001) according to manufacturer's instructions and used to transfect the cells. Test compounds (Merck KGaA, Darmstadt, Germany) were added at concentrations of 20, 60, 80, and 100 μM directly to the well. After 48 h of incubation at 37 $^\circ\text{C}$ and 5% CO_2 , 1 mL of cells (2×10^5) was collected, pelleted, and washed with 1 mL of PBS, before measurement of the luciferase activity using the Luciferase Assay System (Promega, #E1500) according to the manufacturer's instructions ($n = 3$ with 2 replicates in each repetition).

For the adult worm experiments, a 0.4 μM ThinCert cell culture insert (Greiner, #657640) was placed into all wells after cell seeding (including uninfected control wells), and 2 mL of

RPMI 1640 medium (Sigma, #R8758) supplemented with exosome-depleted fetal bovine serum (FBS). (Gibco, #A2720803), 100 U/mL penicillin, and 100 $\mu\text{g}/\text{mL}$ streptomycin was added. ~ 5 adult schistosomes were subsequently added to the inset. Test compounds were then directly added to the insert media in the wells at concentrations of 20, 60, 80, and 100 μM . After 72 h of incubation at 37 $^\circ\text{C}$ and 5% CO_2 , 1 mL (2×10^5) of cells was collected, pelleted, and washed with 1 mL of PBS, before measurement of the luciferase activity using the Luciferase Assay System (Promega, #E1500) according to the manufacturer's instructions ($n = 3$ with 2 replicates in each repetition).

Adult schistosomes were collected from 7-week infected mice by dissecting the hepatic portal vein, with all experiments carried out according to Bavarian animal welfare guidelines, allowance number 02-17-145.

Additionally, 2 mL of cells (4×10^5) was collected, and total RNA was extracted using the GenElute Mammalian Total RNA Miniprep Kit (Sigma-Aldrich, RTN350-1KT). The RNA was DNase treated (New England Biolabs, M0303S), followed by cDNA synthesis using RevertAid Reverse Transcriptase (Thermo Scientific, EP0442). A quantitative real-time PCR (qRT-PCR) analysis of cDNA was conducted using the primers *junb* Forward (Fwd) 5' TCTCTCAAGCTCGCCTC-TTC 3', *junb* Reverse (Rev) 5' ACGTGGTTCATCTTGTG-CAG 3', *gapdh* (Fwd) 5' GGAAGGTGAAGGTCGGAGTC 3', and *gapdh* (Rev) 5' CACAAGCTTCCCGTTCTCAG 3' and iTaq Universal SYBR Green Supermix (BIORAD, 1725120). Values are displayed as $2^{-\Delta\Delta\text{Ct}}$ after normalization to the housekeeping gene *gapdh* and the uninfected control ($n = 2$ with 2 replicates in each repetition).

All data was analyzed in Prism v9.0 using multiple unpaired t tests to assess statistical significance.

ASSOCIATED CONTENT

Supporting Information

The Supporting Information is available free of charge at <https://pubs.acs.org/doi/10.1021/acsinfecdis.2c00360>.

RNA secondary structures; NMR spectra; assessment of the imino proton spectra and ^{19}F screening; results of the fragment screening; syntheses and characterizations; worm assays; miRNA analysis; miR-10-5p quantification; cellular assays (PDF)

AUTHOR INFORMATION

Corresponding Authors

Kamal Azzaoui – Saverna Therapeutics AG, 4123 Allschwil, Switzerland; Email: k.azzaoui@saverna.com

Thomas Spangenberg – Global Health Institute of Merck, Ares Trading S.A., 1262 Eysins, Switzerland; orcid.org/0000-0002-5654-8919; Email: thomas.spangenberg@emdgroup.com

Authors

Youssef Hamway – Institute for Medical Microbiology, Immunology and Hygiene, Technical University of Munich, 81675 Munich, Germany; Center for Global Health, TUM School of Medicine, Technical University of Munich, 81675 Munich, Germany

Kaspar Zimmermann – Saverna Therapeutics AG, 4123 Allschwil, Switzerland

Marcel J. J. Blommers – Saverna Therapeutics AG, 4123 Allschwil, Switzerland

Mariana V. Sousa – Institute for Medical Microbiology, Immunology and Hygiene, Technical University of Munich, 81675 Munich, Germany; Center for Global Health, TUM School of Medicine, Technical University of Munich, 81675 Munich, Germany

Cécile Häberli – Department of Medical Parasitology and Infection Biology, Swiss Tropical and Public Health Institute, 4123 Allschwil, Switzerland; University of Basel, 4001 Basel, Switzerland

Shashank Kulkarni – EMD Serono Research & Development Institute, Inc., Billerica, Massachusetts 01821, United States

Susanna Skalicky – TAmiRNA GmbH, 1110 Wien, Austria

Matthias Hackl – TAmiRNA GmbH, 1110 Wien, Austria

Marjo Götte – Saverna Therapeutics AG, 4123 Allschwil, Switzerland

Jennifer Keiser – Department of Medical Parasitology and Infection Biology, Swiss Tropical and Public Health Institute, 4123 Allschwil, Switzerland; University of Basel, 4001 Basel, Switzerland

Clarissa Prazeres da Costa – Institute for Medical Microbiology, Immunology and Hygiene, Technical University of Munich, 81675 Munich, Germany; Center for Global Health, TUM School of Medicine, Technical University of Munich, 81675 Munich, Germany

Complete contact information is available at:

<https://pubs.acs.org/10.1021/acsinfectdis.2c00360>

Author Contributions

[†]Y.H. and K.Z. contributed equally to the work. Conceptualization: T.S.; K.A.; M.J.J.B. Methodology: S.S.; Y.H.; K.Z.; M.J.J.B.; M.G.; J.K.; C.H.; S.K.; M.V.S.; K.A. Formal analysis: T.S.; Y.H.; C.P.d.C.; M.G.; M.H.; M.J.J.B.; K.A. Writing—original draft: K.A.; T.S.; Y.H. Writing—review and editing: M.H.; J.K.; M.J.J.B.; M.G.; Y.H.; T.S.; K.A. Funding acquisition: T.S. Supervision: T.S.; K.A.

Notes

The authors declare the following competing financial interest(s): S.K. is an employee of EMD Serono Research and Development Institute, Inc., a business of Merck KGaA, Darmstadt, Germany. T.S. is an employee of Ares Trading S.A., an affiliate of Merck KGaA, Darmstadt, Germany. K.Z., M.J.J.B., M.G., and K.A. are employees of Saverna Therapeutics AG. S.S. and M.H. are employees of TAmiRNA GmbH.

ACKNOWLEDGMENTS

Funding from Merck KGaA Darmstadt Germany is gratefully acknowledged. J.K. is grateful to the Swiss National Science Foundation for financial support (No. 320030_175585/1). The table of contents/abstract graphic and Figure 3 were created with [BioRender.com](https://www.bio-render.com).

REFERENCES

- (1) WHO. *WHO guideline on control and elimination of human schistosomiasis*; WHO: Geneva, 2022.
- (2) Angeles, J. M. M.; Mercado, V. J. P.; Rivera, P. T. Behind enemy lines: immunomodulatory armamentarium of the schistosome parasite. *Front. Immunol.* **2020**, *11*, 1018.
- (3) Ofir-Birin, Y.; Regev-Rudzki, N. Extracellular vesicles in parasite survival. *Science* **2019**, *363* (6429), 817–818.

(4) Verjee, M. A. Schistosomiasis: Still a cause of significant morbidity and mortality. *Res. Rep. Trop. Med.* **2019**, *10*, 153–163.

(5) Stroehlein, A. J.; Young, N. D.; Korhonen, P. K.; Hall, R. S.; Jex, A. R.; Webster, B. L.; Rollinson, D.; Brindley, P. J.; Gasser, R. B. The small RNA complement of adult *Schistosoma haematobium*. *PLoS Negl. Trop. Dis.* **2018**, *12* (5), No. e0006535.

(6) Zhu, L.; Liu, J.; Cheng, G. Role of microRNAs in schistosomes and schistosomiasis. *Front. Cell Infect. Microbiol.* **2014**, *4*, 165–165.

(7) Liu, J.; Zhu, L.; Wang, J.; Qiu, L.; Chen, Y.; Davis, R. E.; Cheng, G. *Schistosoma japonicum* extracellular vesicle miRNA cargo regulates host macrophage functions facilitating parasitism. *PLoS Pathog.* **2019**, *15* (6), No. e1007817.

(8) Zhu, L.; Liu, J.; Dao, J.; Lu, K.; Li, H.; Gu, H.; Liu, J.; Feng, X.; Cheng, G. Molecular characterization of *S. japonicum* exosome-like vesicles reveals their regulatory roles in parasite-host interactions. *Sci. Rep.* **2016**, *6*, 25885.

(9) Samoil, V.; Dagenais, M.; Ganapathy, V.; Aldridge, J.; Glebov, A.; Jardim, A.; Ribeiro, P. Vesicle-based secretion in schistosomes: Analysis of protein and microRNA (miRNA) content of exosome-like vesicles derived from *Schistosoma mansoni*. *Sci. Rep.* **2018**, *8* (1), 3286.

(10) Meninger, T.; Barshesht, Y.; Ofir-Birin, Y.; Gold, D.; Brant, B.; Dekel, E.; Sidi, Y.; Schwartz, E.; Regev-Rudzki, N.; Avni, O.; Avni, D. Schistosomal extracellular vesicle-enclosed miRNAs modulate host T helper cell differentiation. *EMBO Rep.* **2020**, *21* (1), No. e47882.

(11) Oh, H.; Ghosh, S. NF- κ B: roles and regulation in different CD4(+) T-cell subsets. *Immunol. Rev.* **2013**, *252* (1), 41–51.

(12) Katagiri, T.; Kameda, H.; Nakano, H.; Yamazaki, S. Regulation of T cell differentiation by the AP-1 transcription factor JunB. *Immunol. Med.* **2021**, *44* (3), 197–203.

(13) Li, B.; Tournier, C.; Davis, R. J.; Flavell, R. A. Regulation of IL-4 expression by the transcription factor JunB during T helper cell differentiation. *EMBO J.* **1999**, *18* (2), 420–432.

(14) Gomard, T.; Michaud, H.-A.; Tempé, D.; Thiolon, K.; Pelegrin, M.; Piechaczyk, M. An NF-kappaB-dependent role for JunB in the induction of proinflammatory cytokines in LPS-activated bone marrow-derived dendritic cells. *PLoS One* **2010**, *5* (3), No. e9585.

(15) Fairfax, K.; Nascimento, M.; Huang, S. C.-C.; Everts, B.; Pearce, E. J. Th2 responses in schistosomiasis. *Semin. Immunopathol.* **2012**, *34* (6), 863–871.

(16) Griffiths-Jones, S.; Saini, H. K.; van Dongen, S.; Enright, A. J. miRBase: tools for microRNA genomics. *Nucleic Acids Res.* **2008**, *36* (Database), D154–D158.

(17) Reuter, J. S.; Mathews, D. H. RNAstructure: software for RNA secondary structure prediction and analysis. *BMC Bioinformatics* **2010**, *11*, 129.

(18) Lorenz, R.; Bernhart, S. H.; Höner Zu Siederdissen, C.; Tafer, H.; Flamm, C.; Stadler, P. F.; Hofacker, I. L. ViennaRNA package 2.0. *Algorithms Mol. Biol.* **2011**, *6*, 26.

(19) Binas, O.; de Jesus, V.; Landgraf, T.; Völklein, A. E.; Martins, J.; Hymon, D.; Kaur Bains, J.; Berg, H.; Biedenbänder, T.; Fürtig, B.; Lakshmi Gande, S.; Niesteruk, A.; Oxenfarth, A.; Shahin Qureshi, N.; Schamber, T.; Schnieders, R.; Tröster, A.; Wacker, A.; Wirmer-Bartoschek, J.; Wirtz Martin, M. A.; Stimal, E.; Azzaoui, K.; Richter, C.; Sreeramulu, S.; José Blommers, M. J.; Schwalbe, H. (19) F NMR-based fragment screening for 14 different biologically active RNAs and 10 DNA and protein counter-screens. *Chembiochem* **2021**, *22* (2), 423–433.

(20) Hajduk, P. J.; Huth, J. R.; Tse, C. Predicting protein druggability. *Drug Discov. Today* **2005**, *10* (23), 1675–1682.

(21) Cox, O. B.; Krojer, T.; Collins, P.; Monteiro, O.; Talon, R.; Bradley, A.; Fedorov, O.; Amin, J.; Marsden, B. D.; Spencer, J.; von Delft, F.; Brennan, P. E. A poised fragment library enables rapid synthetic expansion yielding the first reported inhibitors of PHIP(2), an atypical bromodomain. *Chem. Sci.* **2016**, *7* (3), 2322–2330.

(22) Sreeramulu, S.; Richter, C.; Kuehn, T.; Azzaoui, K.; Blommers, M. J. J.; Del Conte, R.; Fragai, M.; Trieloff, N.; Schmieler, P.; Nazaré, M.; Specker, E.; Ivanov, V.; Oschkinat, H.; Banci, L.; Schwalbe, H. NMR quality control of fragment libraries for screening. *J. Biomol. NMR* **2020**, *74* (10–11), 555–563.

(23) Sreeramulu, S.; Richter, C.; Berg, H.; Wirtz Martin, M. A.; Ceylan, B.; Matzel, T.; Adam, J.; Altincekic, N.; Azzaoui, K.; Bains, J. K.; Blommers, M. J. J.; Ferner, J.; Fürtig, B.; Göbel, M.; Grün, J. T.; Hengesbach, M.; Hohmann, K. F.; Hymon, D.; Knezic, B.; Martins, J. N.; Mertinkus, K. R.; Niesteruk, A.; Peter, S. A.; Pyper, D. J.; Qureshi, N. S.; Scheffer, U.; Schlundt, A.; Schnieders, R.; Stinal, E.; Sudakov, A.; Tröster, A.; Vögele, J.; Wacker, A.; Weigand, J. E.; Wirmer-Bartoschek, J.; Wöhnert, J.; Schwalbe, H. Exploring the druggability of conserved RNA regulatory elements in the SARS-CoV-2 genome. *Angew. Chem., Int. Ed. Engl.* **2021**, *60* (35), 19191–19200.

(24) Vesely, P. W.; Staber, P. B.; Hoefler, G.; Kenner, L. Translational regulation mechanisms of AP-1 proteins. *Mutat. Research* **2009**, *682* (1), 7–12.

(25) McManus, D. P.; Bergquist, R.; Cai, P.; Ranasinghe, S.; Tebeje, B. M.; You, H. Schistosomiasis—from immunopathology to vaccines. *Semin. Immunopathol.* **2020**, *42* (3), 355–371.

(26) Layland, L. E.; Rad, R.; Wagner, H.; da Costa, C. U. Immunopathology in schistosomiasis is controlled by antigen-specific regulatory T cells primed in the presence of TLR2. *Eur. J. Immunol.* **2007**, *37* (8), 2174–2184.

(27) Layland, L. E.; Mages, J.; Loddenkemper, C.; Hoerauf, A.; Wagner, H.; Lang, R.; da Costa, C. U. Pronounced phenotype in activated regulatory T cells during a chronic helminth infection. *J. Immunol.* **2010**, *184* (2), 713–724.

(28) Adams, R. W.; Holroyd, C. M.; Aguilar, J. A.; Nilsson, M.; Morris, G. A. "Perfecting" WATERGATE: clean proton NMR spectra from aqueous solution. *Chem. Commun. (Camb)* **2013**, *49* (4), 358–360.

(29) Griesinger, C.; Otting, G.; Wuethrich, K.; Ernst, R. R. Clean TOCSY for proton spin system identification in macromolecules. *J. Am. Chem. Soc.* **1988**, *110* (23), 7870–7872.

(30) Wijmenga, S. S.; Mooren, M. M. W.; Hilbers, C. W. *NMR of macromolecules: a practical approach*; IRL Press at Oxford University Press, 1993; pp 217–288.